

1 **MTSviewer: a database to visualize mitochondrial targeting sequences, cleavage
2 sites, and mutations on protein structures**

3 Andrew N. Bayne¹, Jing Dong¹, Saeid Amiri², Sali M.K. Farhan^{2,3*}, Jean-François
4 Trempe^{1,*}

5

6 ¹ Department of Pharmacology & Therapeutics and Centre de Recherche en Biologie
7 Structurale, McGill University, Montréal, QC, Canada, H3G 1Y6.

8 ² Department of Neurology and Neurosurgery, Montreal Neurological Institute, McGill
9 University, Montréal, QC, Canada, H4A 3J1.

10 ³ Department of Human Genetics, McGill University, Montréal, QC, Canada, H4A 3J1.

11 * Co-corresponding authors

12

13 Address correspondence to jeanfrancois.trempe@mcgill.ca or sali.farhan@mcgill.ca

14

15

16 **Abstract**

17 **Summary**

18 Mitochondrial dysfunction is implicated in a wide array of human diseases ranging from
19 neurodegenerative disorders to cardiovascular defects. The coordinated localization
20 and import of proteins into mitochondria are essential processes that ensure
21 mitochondrial homeostasis and consequently cell survival. The localization and import
22 of most mitochondrial proteins are driven by N-terminal mitochondrial targeting
23 sequences (MTS's), which interact with import machinery and are removed by the
24 mitochondrial processing peptidase (MPP). The recent discovery of internal MTS's -
25 those which are distributed throughout a protein and act as import regulators or
26 secondary MPP cleavage sites – has expanded the role of both MTS's and MPP
27 beyond conventional N-terminal regulatory pathways. Still, the global mutational
28 landscape of MTS's remains poorly characterized, both from genetic and structural
29 perspectives. To this end, we have integrated a variety of tools into one harmonized
30 R/Shiny database called MTSviewer (<https://neurobioinfo.github.io/MTSvieweR/>) which
31 combines MTS predictions, cleavage sites, genetic variants, pathogenicity predictions,
32 and N-terminomics data with structural visualization using AlphaFold models of human
33 and yeast mitochondrial proteomes.

34 **Availability and Implementation**

35 MTSviewer is freely available on the web at <https://neurobioinfo.github.io/MTSvieweR/>.
36 Source code is available at <https://github.com/neurobioinfo/MTSvieweR>.

37 **Contact**

38 jeanfrancois.trempe@mcgill.ca; sali.farhan@mcgill.ca

39 **Keywords**

40 MTSviewer, variant database, structure visualization, mitochondrial targeting signal,
41 mitochondrial import, cleavage site, MTS

42 **1. Introduction**

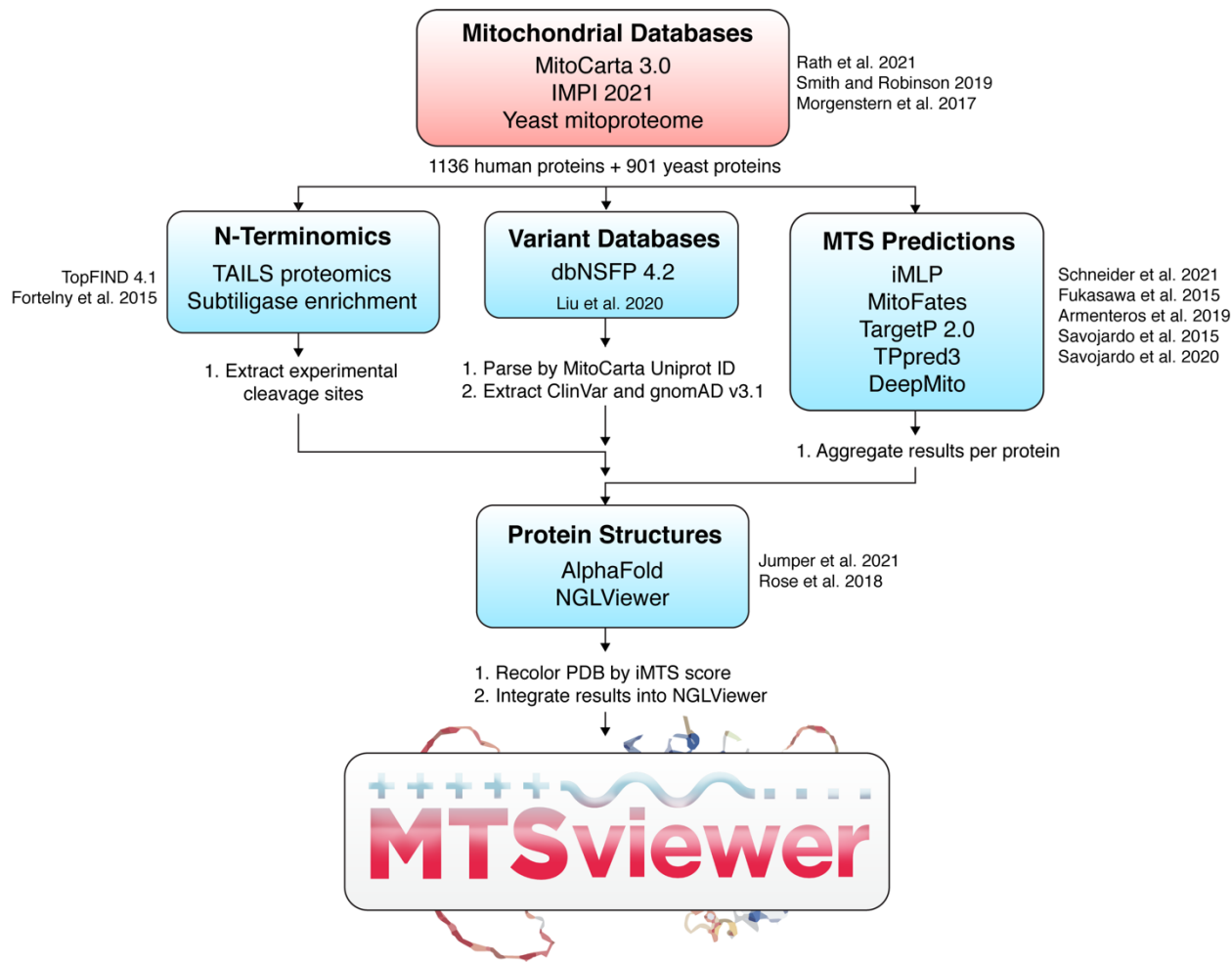
43 Mitochondria are central to organismal health and regulate a diverse array of cellular
44 processes, ranging from energy generation to immunity, proteostasis, and more (Mills et
45 al. 2017; Ruan et al. 2017; Spinelli and Haigis 2018; Pfanner et al. 2019). Even though
46 mitochondria contain their own genome, most mitochondrial proteins are nuclear
47 encoded, translated in the cytosol, and imported into mitochondria (Wiedemann and
48 Pfanner 2017). Consequently, mitochondria have evolved an intricate system of
49 targeting and translocation to import these proteins through translocases of the outer
50 (TOM) and inner (TIM) mitochondrial membranes, and sort them into their correct
51 subcompartment (Neupert 2015). The most common targeting mechanism for matrix-
52 localized proteins utilizes N-terminal mitochondrial targeting sequences (N-MTS), which
53 form amphipathic helices and engage with TOM receptors before being passed through
54 the TIM23 complex into the matrix (Callegari et al. 2020). In the matrix, N-MTS are
55 cleaved off by the mitochondrial processing peptidase (MPP), which acts as a
56 gatekeeper between import and overall mitochondrial quality control (Poveda-Huertes et
57 al. 2017). The breadth of import mechanisms expands considerably when considering
58 proteins localized to the intermembrane space (IMS), which typically lack an N-MTS and
59 rely on disulfide trapping, or transmembrane (TM) proteins, which rely on a combination
60 of accessory machinery and/or MTS's for their insertion and sorting (Hansen and
61 Herrmann 2019). It recently emerged that imported proteins can contain internal MTS's

62 (iMTS), which bind to TOM70 to regulate import rates and may also contain secondary
63 MPP cleavage sites (Backes et al. 2018; Friedl et al. 2020). Furthermore, some proteins
64 lacking an N-MTS still localize to and import into mitochondria via their iMTS's (Bykov et
65 al. 2022; Rahbani et al. 2021).

66 Mitochondrial targeting and import are innately linked to proteolysis, as mitochondria
67 contain more than 40 proteases, coined "mitoproteases", which regulate proteostasis,
68 MTS removal, stress responses, signaling, and more (Deshwal et al. 2020). While MPP
69 is the main protease implicated in N-MTS processing, other proteases act sequentially
70 after MPP cleavage, including MIP, which removes an octapeptide, and XPNPEP3,
71 which removes a single amino acid (Gomez-Fabra Gala and Vögtle 2021). In
72 specialized cases, other mitoproteases can regulate distal cleavages to drive signaling
73 events, including PARL, a rhomboid protease which cleaves TM domains within the
74 inner membrane (Spinazzi and de Strooper 2016; Lysyk et al. 2021). One example of a
75 tandem MPP/PARL-cleaved protein is PINK1, a mitochondrial kinase that relies on its
76 import and processing to either initiate or avoid the mitophagic cascade (Jin et al. 2010;
77 Meissner et al. 2011; Bayne and Trempe 2019).

78 To facilitate the combined study of mitochondrial import and proteolysis, various tools
79 have emerged, namely databases of mitochondrially localized proteins and prediction
80 algorithms for sorting, MTS/iMTS propensity, and cleavage sites. In terms of
81 mitoproteases, mass spectrometry experiments optimized for the labelling and
82 enrichment of newly generated N-termini (neo-N-termini) have provided evidence for
83 both canonical (ie. MTS removal) and non-canonical (ie. distal sites or N-terminal
84 ragging) cleavage events within mitochondria (Calvo et al. 2017; Kleifeld et al. 2011;

85 Vögtle et al. 2009). From a structural perspective, recent work has revealed the
86 structures of human TOM and TIM complexes (Wang et al. 2020b; Qi et al. 2021), and
87 of an iMTS-TOM70 complex between human TOM70 and the SARS-CoV2 protein
88 ORF9b (Jiang et al. 2020). Still, how human MTS's engage with and are passed across
89 the other translocase subunits remain unclear. The structure of human MPP in complex
90 with MTS substrates also remains unknown, which makes it difficult to confidently
91 predict the consequences of MTS variants on MPP processing. From a genetic
92 perspective, comparing the phenotypes of non-synonymous mutations within MTS's,
93 iMTS's, or near cleavage sites may provide key insight into both areas, yet there is no
94 database to facilitate this kind of analysis. There are also currently no resources to
95 rapidly compare the outputs of the numerous mitochondrial prediction algorithms or to
96 visualize MTS's within 3D protein structures. To this end, we hope to expedite the
97 genetic and structural interrogation of human mitochondrial proteins and their MTS's
98 with a novel database: MTSviewer (Fig. 1).



99

100 **Figure 1. Workflow of MTSviewer.** The database construction of MTSviewer, from
101 initial mitochondrial databases to data integration and visualization.

102 **2. Construction and content**

103 The human mitochondrial proteome was downloaded from the MitoCarta 3.0 (1136
104 proteins) (Rath et al. 2021). Additional annotations for the MitoCarta protein list were
105 appended from the Integrated Mitochondrial Protein Index (Q4pre-2021) (Smith and
106 Robinson 2019). The yeast (*Saccharomyces cerevisiae*) mitochondrial proteome was
107 derived from a high confidence dataset (901 proteins) (Morgenstern et al. 2017). Protein
108 sequences were queried by UniProt ID and were submitted to: (1) iMLP – an internal

109 MTS predictor using long short-term memory (LSTM) recurrent neural network
110 architecture (Schneider et al. 2021); (2) TargetP2.0 – a presequence and cleavage site
111 predictor using deep learning and bidirectional LSTM (Almagro Armenteros et al. 2019);
112 (3) MitoFates – a presequence and cleavage site predictor using support vector
113 machine (SVM) classifiers (Fukasawa et al. 2015); (4) TPpred3 – a targeting and
114 cleavage site predictor using Grammatical Restrained Hidden Conditional Random
115 Fields (Savojardo et al. 2015); (5) DeepMito – a sub-mitochondrial localization predictor
116 using deep learning and convoluted neural networks (Savojardo et al. 2020). For
117 cleavage sites derived from N-terminomics, mass spectrometry data were aggregated
118 from TopFIND 4.1 by Uniprot ID of both human and yeast proteins (Fortelny et al.
119 2015). For variants and functional annotations of human proteins, dbNSFP v4.2a was
120 parsed by Uniprot ID against GRCh38/hg38 coordinates (Liu et al. 2020). The resulting
121 list was filtered using an in-house Python script into separate datasets for gnomAD v3.1
122 and ClinVar. Variants unique to the ExAC database were ignored. AlphaFold models for
123 the *Homo sapiens* proteome (UP000005640) and *Saccharomyces cerevisiae*
124 (UP000002311) were downloaded and matched by Uniprot ID (Jumper et al. 2021). An
125 in-house Python script based on BioPandas (Raschka 2017) was used to parse the
126 PDB files and re-color B-factors according to iMTS scores via iMLP. 3D visualization of
127 protein structures was achieved using an adapted version of NGLViewer integrated into
128 our R/Shiny application (Rose et al. 2018).

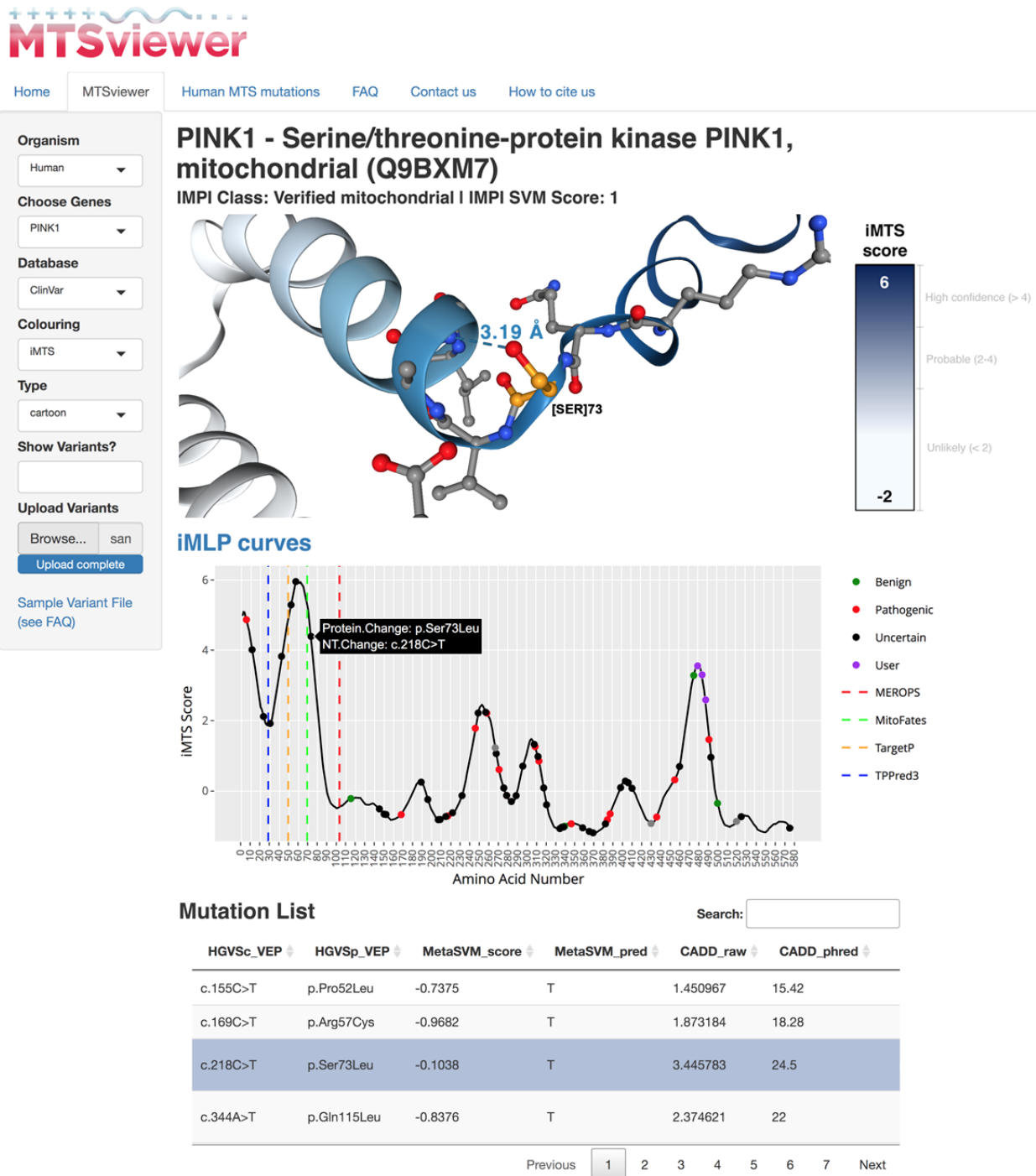
129 **3. Utility and discussion**

130 MTSviewer serves as a user-friendly platform for investigating MTS's from both genetic
131 and structural perspectives. The database requires minimal bioinformatics knowledge

132 and features both human and yeast mitochondrial proteomes. With MTSviewer, users
133 are able to: (1) compare mitochondrial prediction outputs from a variety of algorithms;
134 (2) visualize MTS likelihood on a folded protein structure; (3) compare experimentally
135 identified and predicted proteolytic events; (4) map non-synonymous variants (gnomAD,
136 ClinVar, or user uploaded) within these MTS's and cleavage sites. Using this platform,
137 we have also curated a list of disease-linked variants within human MTS's as a resource
138 for their functional characterization.

139 **User interface**

140 The MTSviewer user interface is intuitive and begins by selecting or searching a gene of
141 interest. Users specify the desired database for variant visualization (currently gnomAD
142 v3.1 or ClinVar), and variants are overlaid onto an XY plot with the iMTS probability
143 from protein N- to C-terminus. Hovering over a variant reveals cursory details which are
144 fully expanded in the variant table. For the structure viewer, two coloring schemes are
145 toggleable: the iMTS score, or the AlphaFold per-residue predicted local distance
146 difference test (pLDDT) confidence score. Users can investigate specific residues or
147 variants by clicking on the iMTS plot or 3D structure, and the structure viewer will
148 automatically highlight the interactions (ie. polar contacts) and residues in proximity (5
149 Å) to the residue of interest (Fig. 2). Users can also upload custom variant lists for their
150 proteins of interest in CSV format, which will be added to the iMTS propensity curve,
151 populated into the variant list data tables, and become visualizable on the 3D protein
152 structure. This feature allows users to compare where their variants lie in terms of MTS
153 propensity, cleavage sites and other pathogenic variants on primary sequence and
154 structural levels.



155

156 **Figure 2. MTSviewer output for PINK1.** A sample output from MTSviewer
157 investigating human PINK1, a mitochondrial kinase with a uniquely long MTS and
158 multiple predicted cleavage sites. Protein sequence, prediction algorithms, and N-

159 terminomics data tables have been omitted for clarity but are available in full on the
160 interactive MTSviewer web server. Ser73Leu has been highlighted as a variant of
161 interest, as Ser73 is found within a region of high MTS propensity near the predicted
162 MitoFates cleavage site.

163 The iMTS plot and structure viewer also contain toggleable visualizations to highlight
164 cleavage site predictions from the various MTS predictors and/or experimentally
165 determined N-terminomics sites. Aggregated comparisons of targeting predictors are
166 pooled in table format, and data frames are exportable to facilitate downstream
167 analyses. Taken together, these features enable users to rapidly generate protein-level
168 hypotheses to test *in vitro*, or to rationalize previous *in vitro* findings with import- or
169 protease-specific context.

170 **PINK1 as a case study**

171 To highlight the utility of MTSviewer we have chosen PINK1 as a case study, given its
172 cryptic N-MTS and the innate coupling of its import and processing to gate its
173 accumulation on the TOM complex. Briefly, PINK1 is known to be cleaved by the
174 rhomboid protease PARL in the IMM at Ala103, which is validated by the N-terminomics
175 outputs seen in MTSviewer. The precise MPP cleavage site within the PINK1 N-MTS
176 remains unknown, though an MPP-cleaved PINK1 fragment accumulates upon PARL
177 knockdown (Greene et al. 2012). Based on the MTSviewer output for PINK1, there are
178 many possibilities for the N-MTS MPP cleavage site, which will be critical to validate
179 using *in vitro* assays, along with the effects of N-MTS variants (eg. Gly30Arg, Pro52Leu,
180 Arg57Cys, and Ser73Leu). While some of these PINK1 N-MTS variants are still cleaved
181 by PARL in healthy mitochondria and accumulate following mitochondrial damage

182 (Sekine et al. 2019), their import rates and effects on MPP processing remain
183 unstudied. Experiments which swap the PINK1 N-MTS with those from other
184 mitochondrial proteins have shown that PINK1 can still be imported into mitochondria
185 with chimeric N-MTS's, though PINK1 accumulation is prevented (Kakade et al. 2022).
186 While many of these N-MTS PINK1 chimeras can still be imported, their specific rates of
187 import have also yet to be measured. This suggests that distal N-MTS elements of
188 mitochondrial proteins (and variants within these regions) will be critical to study beyond
189 the context of binary import success or blockage. Another useful feature of MTSviewer
190 is the ability to gauge the length of a protein's N-MTS by looking at the iMTS propensity
191 plots. For reference, it has been estimated that MTS's are usually 15-50 amino acids
192 long (Wiedemann and Pfanner 2017), yet the PINK1 N-terminus exhibits high MTS
193 propensity across its first 90 amino acids. As all of the MTSviewer iMTS data is
194 available to download, users will be able to analyze global trends in MTS length and
195 propensity across protein families to investigate the downstream consequences of
196 longer or atypical N-MTS's within mitochondrial proteins. Beyond the PINK1 N-MTS, the
197 PINK1 iMTS plot within MTSviewer reveals a putative iMTS within the PINK1 C-
198 terminus (a.a. 460-500), which could regulate PINK1 import or processing rates at the
199 mitochondrial surface. It is known that PINK1 mRNA is co-transported with mitochondria
200 (Harbauer et al. 2022), so it will be important to investigate the role of TOM70 binding to
201 PINK1 and this putative iMTS during translation and import. The MTSviewer output for
202 PINK1 also highlights the need to consider the oligomerization status of proteins when
203 investigating their monomeric AlphaFold structures. PINK1 is known to dimerize on the
204 OMM following depolarization which could occlude its iMTS in the folded dimeric state

205 (Rasool et al. 2022; Okatsu et al. 2013), even if partially unfolded PINK1 monomers
206 could bind to TOM70 upon import. Overall, MTSviewer will guide subsequent studies of
207 atypically targeted proteins like PINK1 in the context of their MTS propensity, cleavage
208 sites, and genetic variants.

209 **Comparison to similar databases**

210 MTSviewer is the first interactive database to bridge genetic variants with mitochondrial
211 targeting predictions, proteolytic evidence, and 3D protein structures. As such, it is
212 essential to highlight the tools and databases that laid the foundation, and to highlight
213 the gaps that our database aims to address. For MTS and MPP cleavage site
214 predictions, TargetP2.0, MitoFates, and TPpred3 utilize orthogonal and sophisticated
215 approaches, yet there remains no harmonized resource to compare their results. Our
216 database currently only features these three predictors, as they are the most recently
217 developed and performed best in benchmarking studies (Imai and Nakai 2020). For raw
218 N-terminomics mass spectrometry data, TopFIND represents the gold standard for data
219 accessibility and cleavage evidence across studies, but it does not provide genetic
220 variants nor structural context for these proteolytic events (Fortelny et al. 2015). In
221 terms of similar 3D structure viewers, the AlphaFold database contains its own module
222 for visualizing contacts of a specified protein but does not allow for significant
223 customizability (Jumper et al. 2021). ICN3D provides another alternative for user
224 uploaded PDB visualization and manipulation, similar in complexity to the standalone
225 PyMOL interface (Wang et al. 2020a). In terms of overall construction, MTSviewer
226 resembles COSMIC-3D, which provides structural visualization for cancer genetics, with
227 a specific focus on the druggability of protein targets (Jubb et al. 2018). KinaseMD has

228 also taken a structural approach to the kinase mutational space, focusing on drug
229 resistance, mutation hotspots, and network rewiring (Hu et al. 2021).

230 **Future developments and limitations**

231 The current construction of MTSviewer features the inherent limitation that N-terminal
232 MTS's within AlphaFold predictions are typically low confidence and are depicted as
233 unstructured. In the future, the inevitable structural determination of human MTS's in
234 complexes with TOM/TIM and/or MPP will enable us to model N-MTS's more accurately
235 and could be integrated as a scoring metric or docking module into later versions of
236 MTSviewer. We will also implement a module for protease-specific exports (ie. variant
237 lists near protease sites) to assess enrichment of pathogenic or uncharacterized
238 variants near proteolytic sites. Overall, MTSviewer will be updated with new MTS
239 prediction algorithms, experimental proteolytic evidence, and updated AlphaFold
240 models on a regular basis.

241 **4. Conclusions**

242 MTSviewer is a novel R/Shiny database for investigating the mutational space, targeting
243 sequences, proteolysis, and 3D structures of mitochondrial proteins. Users require
244 minimal bioinformatics training and can rapidly generate variant lists, investigate
245 structural consequences, compare the results of various mitochondrial prediction tools,
246 and dissect potential cleavage sites.

247 **Declarations**

248 **Ethics approval and consent to participate**

249 Not applicable

250 **Consent for publication**

251 Not applicable

252 **Availability of data and materials**

253 The MTSviewer database is freely accessible via

254 <https://neurobioinfo.github.io/MTSvieweR/>. Source code is available at

255 <https://github.com/neurobioinfo/MTSvieweR>.

256 **Competing interests**

257 The authors declare that they have no competing interests

258 **Funding**

259 A.N.B. is supported by a Canadian Institutes for Health Research (CIHR) Doctoral

260 Fellowship. J.D is supported by a CIHR Canada Graduate Scholarship. This work was

261 supported by a Canada Research Chair (Tier 2) in Structural Pharmacology to J.-F.T.,

262 as well as a Discovery Grant from the Natural Sciences and Engineering Research

263 Council (NSERC) of Canada (RGPIN-2022-04042).

264 **Authors' contributions**

265 A.N.B. and J.F.T conceptualized MTSviewer. A.N.B., J.D., and S.A. created the original

266 R/Shiny and Python codes used in database construction. All authors contributed to

267 feature development, troubleshooting, and optimization of the database functionalities.

268 A.N.B and J.F.T wrote the manuscript with contributions and editing from J.D., S.A., and

269 S.F. All authors read and approved the final manuscript.

270 **Acknowledgements**

271 We would like to thank Niels van der Velden for the ongoing support with NGLVieweR
272 scripting and integration.

273 **References**

274 Armenteros A, Emanuelsson SM, Winther O, Von Heijne O, Elofsson G. Detecting
275 sequence signals in targeting peptides using deep learning. Life Science Alliance.
276 2019;2.

277 Backes S, Hess S, Boos F, Woellhaf MW, Gödel S, Jung M, et al. Tom70 enhances
278 mitochondrial preprotein import efficiency by binding to internal targeting sequences. *J
279 Cell Biol.* 2018;217:1369–82.

280 Bayne AN, Trempe J-F. Mechanisms of PINK1, ubiquitin and Parkin interactions in
281 mitochondrial quality control and beyond. *Cell Mol Life Sci.* 2019;76:4589–611.

282 Bykov YS, Flohr T, Boos F, Zung N, Herrmann JM, Schuldiner M. Widespread use of
283 unconventional targeting signals in mitochondrial ribosome proteins. *EMBO J.*
284 2022;41:e109519.

285 Callegari S, Cruz-Zaragoza LD, Rehling P. From TOM to the TIM23 complex - handing
286 over of a precursor. *Biol Chem.* 2020;401:709–21.

287 Calvo SE, Julien O, Clauser KR, Shen H, Kamer KJ, Wells JA, et al. Comparative
288 analysis of mitochondrial N-termini from mouse, human, and yeast. *Mol Cell
289 Proteomics.* 2017;16:512–23.

290 Deshwal S, Fiedler KU, Langer T. Mitochondrial proteases: Multifaceted regulators of
291 mitochondrial plasticity. *Annu Rev Biochem.* 2020;89:501–28.

292 Fortelny N, Yang S, Pavlidis P, Lange PF, Overall CM. Proteome TopFIND 3.0 with
293 TopFINDer and PathFINDer: database and analysis tools for the association of protein
294 termini to pre- and post-translational events. *Nucleic Acids Res.* 2015;43 Database
295 issue:D290-7.

296 Friedl J, Knopp MR, Groh C, Paz E, Gould SB, Herrmann JM, et al. More than just a
297 ticket canceller: the mitochondrial processing peptidase tailors complex precursor
298 proteins at internal cleavage sites. *Mol Biol Cell.* 2020;31:2657–68.

299 Fukasawa Y, Tsuji J, Fu S-C, Tomii K, Horton P, Imai K. MitoFates: Improved Prediction
300 of Mitochondrial Targeting Sequences and Their Cleavage Sites*. *Molecular & Cellular
301 Proteomics.* 2015;14:1113–26.

302 Gomez-Fabra Gala M, Vögtle F-N. Mitochondrial proteases in human diseases. *FEBS
303 Lett.* 2021;595:1205–22.

304 Greene AW, Grenier K, Aguilera MA, Muise S, Farazifard R, Haque ME, et al.
305 Mitochondrial processing peptidase regulates PINK1 processing, import and Parkin
306 recruitment. *EMBO Rep.* 2012;13:378–85.

307 Hansen KG, Herrmann JM. Transport of proteins into mitochondria. *Protein J.*
308 2019;38:330–42.

309 Harbauer AB, Hees JT, Wanderoy S, Segura I, Gibbs W, Cheng Y, et al. Neuronal
310 mitochondria transport Pink1 mRNA via synaptosomal 2 to support local mitophagy.
311 *Neuron.* 2022;110:1516-1531.e9.

312 Hu R, Xu H, Jia P, Zhao Z. KinaseMD: kinase mutations and drug response database.
313 *Nucleic Acids Res.* 2021;49:D552–61.

314 Imai K, Nakai K. Tools for the recognition of sorting signals and the prediction of
315 subcellular localization of proteins from their amino acid sequences. *Front Genet.*
316 2020;11:607812.

317 Jiang H-W, Zhang H-N, Meng Q-F, Xie J, Li Y, Chen H, et al. SARS-CoV-2 Orf9b
318 suppresses type I interferon responses by targeting TOM70. *Cell Mol Immunol.*
319 2020;17:998–1000.

320 Jin SM, Lazarou M, Wang C, Kane LA, Narendra DP, Youle RJ. Mitochondrial
321 membrane potential regulates PINK1 import and proteolytic destabilization by PARL. *J
322 Cell Biol.* 2010;191:933–42.

323 Jubb HC, Saini HK, Verdonk ML, Forbes SA. COSMIC-3D provides structural
324 perspectives on cancer genetics for drug discovery. *Nat Genet.* 2018;50:1200–2.

325 Jumper J, Evans R, Pritzel A, Green T, Figurnov M, Ronneberger O, et al. Highly
326 accurate protein structure prediction with AlphaFold. *Nature.* 2021;596:583–9.

327 Kakade P, Ojha H, Raimi OG, Shaw A, Waddell AD, Ault JR, et al. Mapping of a N-
328 terminal α -helix domain required for human PINK1 stabilization, Serine228
329 autophosphorylation and activation in cells. *Open Biol.* 2022;12:210264.

330 Kleifeld O, Doucet A, Prudova A, auf dem Keller U, Gioia M, Kizhakkedathu JN, et al.
331 Identifying and quantifying proteolytic events and the natural N terminome by terminal
332 amine isotopic labeling of substrates. *Nat Protoc.* 2011;6:1578–611.

333 Liu X, Li C, Mou C, Dong Y, Tu Y. dbNSFP v4: a comprehensive database of transcript-
334 specific functional predictions and annotations for human nonsynonymous and splice-
335 site SNVs. *Genome Med.* 2020;12:103.

336 Lysyk L, Brassard R, Arutyunova E, Siebert V, Jiang Z, Takyi E, et al. Insights into the
337 catalytic properties of the mitochondrial rhomboid protease PARL. *J Biol Chem.*
338 2021;296:100383.

339 Meissner C, Lorenz H, Weihofen A, Selkoe DJ, Lemberg MK. The mitochondrial
340 intramembrane protease PARL cleaves human Pink1 to regulate Pink1 trafficking:
341 Rhomboid protease PARL cleaves human Pink1. *J Neurochem.* 2011;117:856–67.

342 Morgenstern M, Stiller SB, Lübbert P, Peikert CD, Dannenmaier S, Drepper F, et al.
343 Definition of a high-confidence mitochondrial proteome at quantitative scale. *Cell Rep.*
344 2017;19:2836–52.

345 Mills EL, Kelly B, O'Neill LAJ. Mitochondria are the powerhouses of immunity. *Nat*
346 *Immunol.* 2017;18:488–98.

347 Neupert W. A perspective on transport of proteins into mitochondria: a myriad of open
348 questions. *J Mol Biol.* 2015;427 6 Pt A:1135–58.

349 Okatsu K, Uno M, Koyano F, Go E, Kimura M, Oka T, et al. A dimeric PINK1-containing
350 complex on depolarized mitochondria stimulates Parkin recruitment. *J Biol Chem.*
351 2013;288:36372–84.

352 Pfanner N, Warscheid B, Wiedemann N. Mitochondrial proteins: from biogenesis to
353 functional networks. *Nat Rev Mol Cell Biol.* 2019;20:267–84.

354 Poveda-Huertes D, Mulica P, Vögtle FN. The versatility of the mitochondrial
355 presequence processing machinery: cleavage, quality control and turnover. *Cell Tissue*
356 *Res.* 2017;367:73–81.

357 Qi L, Wang Q, Guan Z, Wu Y, Shen C, Hong S, et al. Cryo-EM structure of the human
358 mitochondrial translocase TIM22 complex. *Cell Res.* 2021;31:369–72.

359 Rahbani JF, Roesler A, Hussain MF, Samborska B, Dykstra CB, Tsai L, et al. Creatine
360 kinase B controls futile creatine cycling in thermogenic fat. *Nature.* 2021;590:480–5.

361 Raschka S. BioPandas: Working with molecular structures in pandas DataFrames. *J*
362 *Open Source Softw.* 2017;2:279.

363 Rasool S, Veyron S, Soya N, Eldeeb MA, Lukacs GL, Fon EA, et al. Mechanism of
364 PINK1 activation by autophosphorylation and insights into assembly on the TOM
365 complex. *Mol Cell.* 2022;82:44-59.e6.

366 Rath S, Sharma R, Gupta R, Ast T, Chan C, Durham TJ. 0: an updated mitochondrial
367 proteome now with sub-organelle localization and pathway annotations. *Nucleic Acids*
368 *Research.* 2021;49:D1541-1547.

369 Rose AS, Bradley AR, Valasatava Y, Duarte JM, Prlic A, Rose PW. NGL viewer: web-
370 based molecular graphics for large complexes. *Bioinformatics.* 2018;34:3755–8.

371 Ruan L, Zhou C, Jin E, Kucharavy A, Zhang Y, Wen Z, et al. Cytosolic proteostasis
372 through importing of misfolded proteins into mitochondria. *Nature.* 2017;543:443–6.

373 Savojardo C, Bruciaferri N, Tartari G, Martelli PL, Casadio R. DeepMito: accurate
374 prediction of protein sub-mitochondrial localization using convolutional neural networks.
375 *Bioinformatics.* 2020;36:56–64.

376 Savojardo C, Martelli PL, Fariselli P, Casadio R. TPpred3 detects and discriminates
377 mitochondrial and chloroplastic targeting peptides in eukaryotic proteins. *Bioinformatics.*
378 2015;31:3269–75.

379 Sekine S, Wang C, Sideris DP, Bunker E, Zhang Z, Youle RJ. Reciprocal roles of Tom7
380 and OMA1 during mitochondrial import and activation of PINK1. *Mol Cell*.
381 2019;73:1028-1043.e5.

382 Schneider K, Zimmer D, Nielsen H, Herrmann JM, Mühlhaus T. iMLP, a predictor for
383 internal matrix targeting-like sequences in mitochondrial proteins. *Biological Chemistry*.
384 2021;402:937–43.

385 Smith AC, Robinson AJ. MitoMiner v4.0: an updated database of mitochondrial
386 localization evidence, phenotypes and diseases. *Nucleic Acids Res*. 2019;47:D1225–8.

387 Spinazzi M, Strooper D. PARL: The mitochondrial rhomboid protease. *Seminars in Cell*
388 & Developmental Biology

389 Spinelli JB, Haigis MC. The multifaceted contributions of mitochondria to cellular
390 metabolism. *Nat Cell Biol*. 2018;20:745–54.

391 Vögtle F-N, Wortelkamp S, Zahedi RP, Becker D, Leidhold C, Gevaert K, et al. Global
392 analysis of the mitochondrial N-proteome identifies a processing peptidase critical for
393 protein stability. *Cell*. 2009;139:428–39.

394 Wang J, Youkharibache P, Zhang D, Lanczycki CJ, Geer RC, Madej T, et al. iCn3D, a
395 web-based 3D viewer for sharing 1D/2D/3D representations of biomolecular structures.
396 *Bioinformatics*. 2020a;36:131–5.

397 Wang W, Chen X, Zhang L, Yi J, Ma Q, Yin J, et al. Atomic structure of human TOM
398 core complex. *Cell Discov*. 2020b;6:67.

399 Wiedemann N, Pfanner N. Mitochondrial machineries for protein import and assembly.
400 *Annu Rev Biochem*. 2017;86:685–714.